Neutrino oscillations

The discovery that neutrinos can change their types (flavours) while traveling in space, indicating they have non-zero masses was one of the breakthrough moments in elementary particle physics. It proved that the Standard Model of particles and their strong and electroweak interactions is not a complete theory, because it does not provide mechanism for generating neutrino masses. The first hypothesis about neutrino oscillations was formulated by Bruno Pontecorvo in 1957, who suggested the possibility of neutrino-antineutrino oscillations [97]. After discovery of second type of neutrino, ν_μ, Maki, Nakagawa and Sakata discussed the possibility that ν_e and ν_μ can be a mixture of two neutrino mass eigenstates [98]. Finally, the first model of $\nu_e \longleftrightarrow \nu_\mu$ oscillations was formulated by Pontecorvo [99] in 1968 and later developed by Gribov and Pontecorvo [100] in 1969. The work included in the publication from 1969 was motivated by the results from the first experiment that was searching for neutrinos from the Sun. The first neutrino detector designed to study solar neutrinos was constructed in the Homestake gold mine in South Dakota by Raymond Davis Jr. It was filled with 615 t of tetrachloroethylene and was designed to detect solar neutrinos in the reaction:

$$\nu_e + {}^{37}\mathrm{Cl} \to {}^{37}\mathrm{Ar} + \mathrm{e}^-. \tag{2.1}$$

The first results from Davis' experiment, published in 1968 [21] indicated that the number of interactions of ν_e from the Sun is much smaller than theoretically expected. In the final publication [22] the quoted flux of solar neutrinos measured in the experiment was

$$2.56 \pm 0.16(\mathrm{stat}) \pm 0.16(\mathrm{sys})\ \mathrm{SNU}, \tag{2.2}$$

where SNU stands for Solar Neutrino Unit (reaction per 10^{36} target atoms per second). This result corresponds to about 30% of the flux predicted by the Solar Standard Model 8.5 ± 0.9 SNU [102]. Pontecorvo and Gribov postulated that the number of detected ν_e is smaller than expected because electron neutrinos can change the flavour (oscillate) into muon neutrinos, $\nu_e \rightleftarrows \nu_\mu$, on their way to the Earth. The oscillation hypothesis was confirmed in 1998 by the Super-Kamiokande experiment [3] that studied interactions of neutrinos produced when primary cosmic rays (mostly protons) interact with the atmosphere. The flux of atmospheric neutrinos was measured by observing leptons produced in interactions of neutrinos on nuclei (Eq. (2.3)):

$$\nu + \mathrm{N} \to \mathrm{l} + \mathrm{X}, \tag{2.3}$$

where ν is either neutrino or antineutrino ($\nu_e, \nu_\mu, \overline{\nu}_e, \overline{\nu}_\mu$), N is nucleus, l is lepton, and X stands for produced hadrons. Super-Kamiokande is the 50 kt water Cherenkov detector that can distinguish
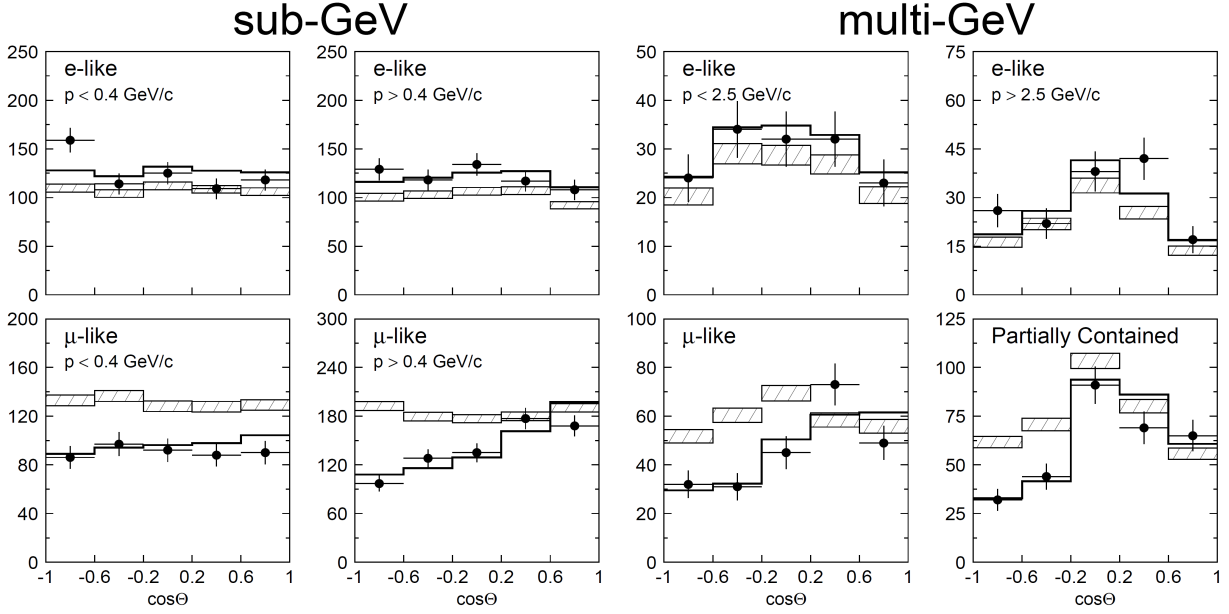
Figure 2.1. Results of Super-Kamiokande analysis of atmospheric neutrinos. Zenith angle distributions of e-like and μ-like events for lower-energy (sub-GeV) and higher-energy (multi-GeV) data samples. Comparison of data (solid points), Monte Carlo expectations assuming no oscillations (hatched region, statistical errors) and results of the best fit of $\nu_\mu \to \nu_\tau$ two-flavour oscillation model (bold line) with the flux normalization fitted as a free parameter. Multi-GeV μ-like distributions are shown separately for events fully contained and partially contained in the detector (two bottom-right plots). Image from [3].

muons from electrons but is not able to distinguish their charge and consequently neutrinos from antineutrinos. The experiment reported a deficit of $\nu_\mu(\overline{\nu}_\mu)$ strongly varying with zenith angle[1] θ in accordance with the two-flavour $\nu_\mu \to \nu_\tau$ oscillation model (Fig. 2.1). The largest deficit was observed for upward-going muons with $\cos\theta < 0$.

In the years 2001 [4] and 2002 [5], the solar neutrino deficit was finally explained by the researchers from the Sudbury Neutrino Observatory (SNO) experiment led by Arthur B. McDonald. They published evidence that total flux of neutrinos from the Sun is in agreement with the predictions of the Solar Standard Model. The SNO detector was filled with 1 kt of ultra pure heavy water (D_2O) and allowed for detection of the solar neutrinos via the reactions

$$\nu_e + D \to e^- + p + p \ (\text{CC}), \tag{2.4}$$

$$\nu_x + D \to \nu_x + p + n \ (\text{NC}), \tag{2.5}$$

$$\nu_x + e^- \to \nu_x + e^- \ (\text{ES}). \tag{2.6}$$

Charged-current reactions (CC) (Eq. (2.4)) were sensitive only to ν_e and therefore provided the flux of electron neutrinos, while neutral-current reactions (NC) were equally sensitive to ν_e, ν_μ and ν_τ and measured the total neutrino flux. Additionally, elastic-scattering (ES) reaction, predominantly sensitive to ν_e, provided the information about the direction of the neutrino. The final SNO measurement [24] of ^{8}B solar neutrino flux is

$$\phi = 5.25 \pm 0.16(\text{stat})^{+0.11}_{-0.13}(\text{sys}) \times 10^6 \ \text{cm}^{-2} \ \text{s}^{-1}. \tag{2.7}$$

The above result is in good agreement with predictions from Standard Solar Models [1, 2].

---

[1] θ is an angle between direction of lepton and local vertical line.

The physicists: Takaaki Kajita leading the oscillation analysis in the Super-Kamiokande collaboration and Arthur B. McDonald from the SNO collaboration were awarded the Nobel Prize in Physics in 2015 for their leading role in "the discovery of neutrino oscillations, which shows that neutrinos have mass", while Raymond Davis Jr was awarded the Nobel Prize in 2002 for the detection of solar neutrinos.

2.1. Three-flavour oscillations

Neutrino oscillation model [124, 129] describes the phenomenon that neutrinos can change their types while traveling in space. In that model neutrinos of definite flavour produced in the weak interactions are superpositions of the mass eigenstates

$$|\nu_\alpha\rangle = \sum_{j=1}^{3} U^*_{\alpha j}|\nu_j\rangle, \tag{2.8}$$

where ν_α is a neutrino of flavour α = e, μ or τ, ν_j is a neutrino of definitive mass m_j, and U is the PMNS (Pontecorvo–Maki–Nakagawa–Sakata) leptonic mixing matrix. Similarly, every neutrino mass eigenstate $|\nu_j\rangle$ is the superposition of the states of definite flavour, $|\nu_\alpha\rangle$:

$$|\nu_j\rangle = \sum_{\alpha=e,\mu,\tau} U_{\alpha j}|\nu_\alpha\rangle. \tag{2.9}$$

Assuming that there are only three neutrino flavours, **U** is 3×3 matrix, and can be written as

$$\mathbf{U} = \begin{pmatrix} U_{e1} & U_{e2} & U_{e3} \\ U_{\mu 1} & U_{\mu 2} & U_{\mu 3} \\ U_{\tau 1} & U_{\tau 2} & U_{\tau 3} \end{pmatrix}. \tag{2.10}$$

In the Standard Model, mixing matrix **U** is unitary. However, if there are additional sterile neutrinos that do not couple to Z or W boson (see Section 2.2), then the **U** matrix would be a submatrix of bigger $N \times N$ matrix and would not be unitary.

Squared elements of the **U** matrix, $|U_{\alpha j}|^2$, describe the neutrino flavour-α fraction of ν_j (Fig. 2.2).
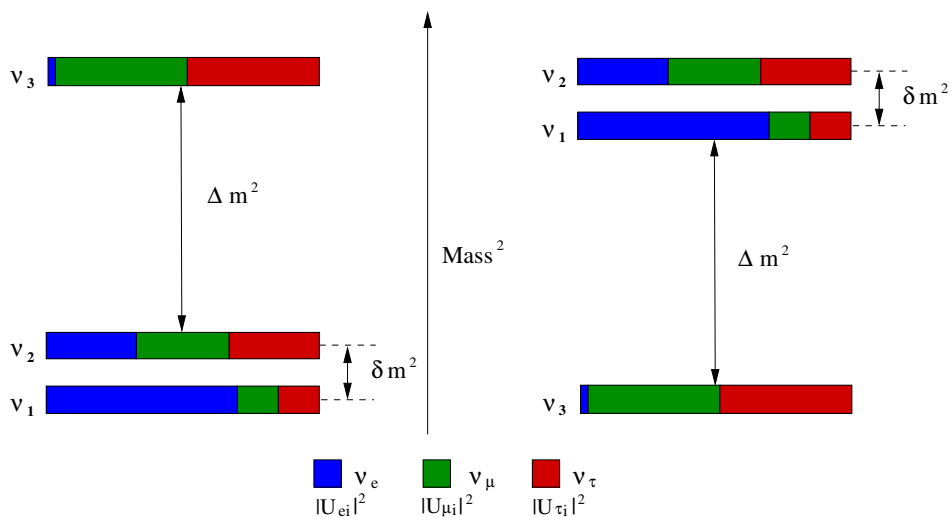

Figure 2.2. Neutrino mass states as the combination of known flavour states. Left plot: normal mass hierarchy (ν_1 and ν_2 states have lower mass than ν_3). Right plot: inverted mass hierarchy. Squares of the elements of mixing matrix **U**, $|U_{\alpha i}|^2$, describe flavour-α fractions of ν_i.

Below, the 3σ C.L. (confidence level) ranges of the elements of the three-flavour mixing matrix $\mathbf{U}$, as derived from the three-neutrino fit based on data available in May 2016 (NuFIT 2.1) [121, 122], are shown:

$$|\mathbf{U}| = \begin{pmatrix} 0.798 - 0.843 & 0.517 - 0.584 & 0.137 - 0.158 \\ 0.232 - 0.520 & 0.445 - 0.697 & 0.617 - 0.789 \\ 0.249 - 0.529 & 0.462 - 0.708 & 0.597 - 0.773 \end{pmatrix}. \tag{2.11}$$

The numbers were produced under the assumption that the matrix $\mathbf{U}$ is unitary.

The PMNS matrix can be parameterized by introducing three mixing angles θ_{ij} and CP-violating phase δ. Symbol s_{ij} stands for $\sin\theta_{ij}$ and $c_{ij} = \cos\theta_{ij}$:

$$\mathbf{U} = \begin{pmatrix} c_{12}c_{13} & s_{12}c_{13} & s_{13}e^{-i\delta} \\ -s_{12}c_{23} - c_{12}s_{23}s_{13}e^{i\delta} & c_{12}c_{23} - s_{12}s_{23}s_{13}e^{i\delta} & s_{23}c_{13} \\ s_{12}s_{23} - c_{12}c_{23}s_{13}e^{i\delta} & -c_{12}s_{23} - s_{12}c_{23}s_{13}e^{i\delta} & c_{23}c_{13} \end{pmatrix}. \tag{2.12}$$

The matrix can also be rewritten as the product of the matrices shown below. Forth matrix has to be added if neutrino is of Majorana (see Section 2.3) type. In this case two additional CP-violating phases η and κ have to be introduced,

$$\mathbf{U} = \begin{pmatrix} 1 & 0 & 0 \\ 0 & c_{23} & s_{23} \\ 0 & -s_{23} & c_{23} \end{pmatrix} \begin{pmatrix} c_{13} & 0 & s_{13}e^{-i\delta} \\ 0 & 1 & 0 \\ -s_{13}e^{i\delta} & 0 & c_{13} \end{pmatrix} \begin{pmatrix} c_{12} & s_{12} & 0 \\ -s_{12} & c_{12} & 0 \\ 0 & 0 & 1 \end{pmatrix} \begin{pmatrix} 1 & 0 & 0 \\ 0 & e^{i\eta} & 0 \\ 0 & 0 & e^{i\kappa} \end{pmatrix}. \tag{2.13}$$

The PMNS matrix can be used to calculate the probability that the neutrino of energy E, produced as neutrino of flavour α, interacts as neutrino of flavour β after traveling in vacuum at the distance L from a production point to the detector. The amplitude of the $\nu_\alpha \to \nu_\beta$ transition is given by

$$A = \sum_j U_{\alpha j}^* e^{\frac{-im_j^2 L}{2E}} U_{\beta j}, \tag{2.14}$$

and shown in the diagram in Fig. 2.3. Probability of transition $\nu_\alpha \to \nu_\beta$ in vacuum is obtained by squaring of the amplitude A

$$\begin{aligned} P_{\nu_\alpha \to \nu_\beta}(L, E) &= |A|^2 \\ &= \delta_{\alpha\beta} - 4\sum_{j>k} \Re\mathfrak{e}(U_{\alpha j}^* U_{\beta j} U_{\alpha k} U_{\beta k}^*) \sin^2\left(\frac{\Delta m_{jk}^2 L}{4E}\right) \\ &\quad + 2\sum_{j>k} \Im\mathfrak{m}(U_{\alpha j}^* U_{\beta j} U_{\alpha k} U_{\beta k}^*) \sin\left(\frac{\Delta m_{jk}^2 L}{2E}\right). \end{aligned} \tag{2.15}$$

To obtain Eq. (2.15), the unitarity of $\mathbf{U}$ matrix was assumed. The $\Delta m_{jk}^2 \equiv m_j^2 - m_k^2$ is the splitting between the squared masses of ν_j and ν_k. It can be deduced from Eq. (2.15) that oscillation from flavour α to β implies nonzero Δm_{jk}^2 and therefore nonzero neutrino masses. The quantity

$$\frac{\Delta m_{jk}^2 L}{4E}, \tag{2.16}$$

on which the oscillation depends, can be written in a different form:

$$1.27\frac{\Delta m_{jk}^2(\text{eV}^2)L(\text{km})}{E(\text{GeV})}, \tag{2.17}$$
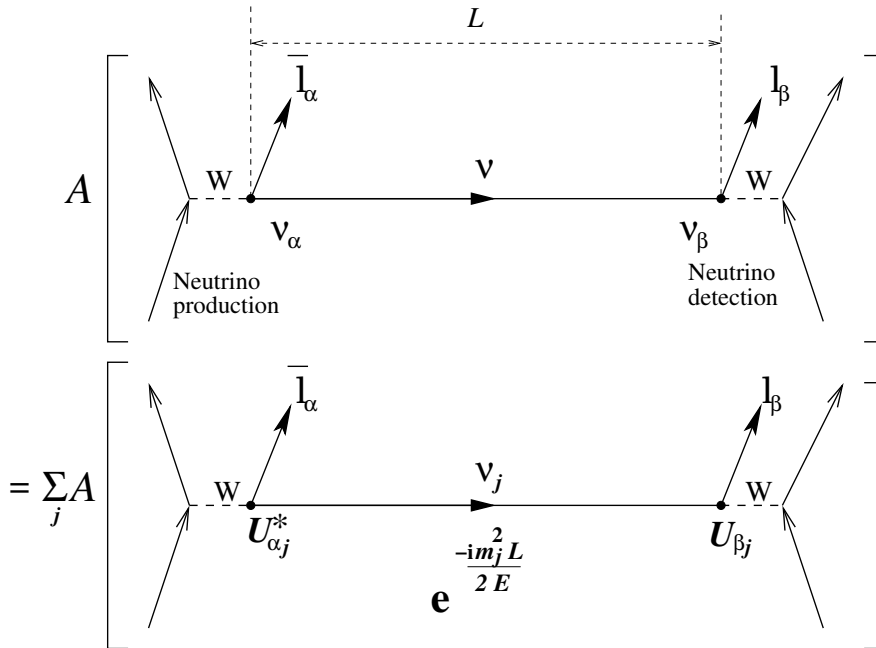
Figure 2.3. Amplitude A of the neutrino oscillations in vacuum. The figure is based on the diagram from [124].

if one inserts into the formula $\hbar$ and c factors omitted before. Therefore $\sin^2\left(\frac{\Delta m_{jk}^2 L}{4E}\right)$ becomes $\sin^2\left(1.27\frac{\Delta m_{jk}^2 L}{E}\right)$. It has been found experimentally that $\Delta m_{12}^2 \equiv \delta m^2$ $(\simeq 7.5 \times 10^{-5}~\text{eV}^2)$ is much smaller than $\Delta m_{32}^2 \simeq \Delta m_{31}^2 \equiv \Delta m^2$ $(\simeq 2.4 \times 10^{-3}~\text{eV}^2)$ (Fig. 2.2)[1].

In the long-baseline accelerator experiments like MINOS+, the main detector is located several hundred kilometers from the neutrino source and energies of neutrinos from the beam are in the GeV region. In such experiments the oscillations are driven by the larger mass-squared difference Δm^2. It is also known from the reactor [17–19] and accelerator [27, 28] experiments that θ_{13} parameter, responsible for the appearance of ν_e in the beam of ν_μ, is small. Therefore, ν_μ are expected to turn mostly into ν_τ and many features of the data can be described by an effective two-flavour model. Probabilities of survival of muon neutrinos and appearance of tau neutrinos can be approximated by the two-flavour formulae

$$P_{\nu_\mu \to \nu_\mu} \approx 1 - \sin^2 2\theta \sin^2\left(\frac{\Delta m^2 L}{4E}\right) \tag{2.18}$$

and

$$P_{\nu_\mu \to \nu_\tau} \approx \sin^2 2\theta \sin^2\left(\frac{\Delta m^2 L}{4E}\right). \tag{2.19}$$

In the three-flavour framework, oscillation probabilities depend on all the mixing parameters. The leading order probabilities of survival of muon neutrinos in vacuum can be written in the same form as in the two-flavour approximation (Eq. (2.18)) with the effective mixing angle and Δm^2 given by [13]:

---

[1]Detailed ranges of oscillation parameters allowed by existing neutrino data being the result of fit [122] to these data are presented in Appendix A.

$$\sin^2 2\theta = 4\sin^2\theta_{23}\cos^2\theta_{13}(1 - \sin^2\theta_{23}\cos^2\theta_{13}),$$
$$\Delta m^2 = \Delta m_{32}^2 + \Delta m_{21}^2 \sin^2\theta_{12} \qquad\qquad (2.20)$$
$$+ \Delta m_{21}^2 \cos\delta_{\mathrm{CP}} \sin\theta_{13} \tan\theta_{23} \sin 2\theta_{12}.$$

For neutrinos propagating in matter, oscillation probabilities can be substantially modified due to the coherent forward elastic scattering of the neutrinos from the particles they encounter in the medium [29]. Neutrino of any flavour (ν_e, ν_μ and ν_τ) traveling through matter can exchange a Z boson with an electron or a nucleon. On the contrary, only ν_e can exchange a W boson with an electron, and this difference between interactions with matter of ν_e and other neutrino flavours gives rise to the modification of neutrino oscillations. As a result of the coherent forward scattering of neutrino with matter, the energy E of neutrino state becomes $E + V$, where V is an interaction potential energy. The V can be $V_{\mathrm{W}} = \sqrt{2}G_{\mathrm{F}}n_e$ being the result of the scattering of ν_e via W exchange or $V_{\mathrm{Z}} = -\frac{1}{2}\sqrt{2}G_{\mathrm{F}}n_n$ related to the Z boson exchange. The V_{Z} affects all neutrino flavours equally and therefore has no impact on oscillations. Here, G_{F} is the Fermi weak coupling constant, and n_e and n_n are the electron and neutron densities in matter. Assuming two-neutrino case, with one neutrino being ν_e, the probability of transition of one flavour state into another can be written in the two-flavour form:

$$\mathrm{P_M} = \sin^2(2\theta_{\mathrm{M}}) \sin^2\left(\frac{\Delta m_{\mathrm{M}}^2 L}{4E}\right), \qquad\qquad (2.21)$$

with vacuum parameters θ and Δm^2 replaced by their in-matter equivalents:

$$\sin^2 2\theta_{\mathrm{M}} \equiv \frac{\sin^2 2\theta}{\sin^2 2\theta + (A - \cos 2\theta)^2} \qquad\qquad (2.22)$$

and

$$\Delta m_{\mathrm{M}}^2 \equiv \Delta m^2 \sqrt{\sin^2 2\theta + (A - \cos 2\theta)^2}, \qquad\qquad (2.23)$$

with matter effects described by the parameter A:

$$A \equiv \frac{V_{\mathrm{W}}/2}{\Delta m^2/4E} = \frac{2\sqrt{2}G_{\mathrm{F}}n_e E}{\Delta m_{31}^2}. \qquad\qquad (2.24)$$

The sign of V is positive for neutrinos and negative for antineutrinos. Consequently, in the expressions on Δm_{M}^2 and $\sin^2 2\theta_{\mathrm{M}}$, a measure of importance of the matter effects – quantity A, has to be replaced by $-A$ and there is a difference between oscillation probabilities for neutrinos and antineutrinos propagating in matter. In the long-baseline accelerator neutrino experiments, matter effects play the biggest role in the study of appearance of electron neutrinos in the beam of muon neutrinos. In the study of ν_μ disappearance or ν_τ appearance matter effects are negligible.

In Figs. 2.4 and 2.5, exact, not approximated standard oscillation probabilities for transitions $\nu_\mu \to \nu_\tau$, $\nu_\mu \to \nu_e$, together with probability that ν_μ does not change its type are plotted as a function of L/E. Probabilities in Fig. 2.4 are for single neutrino energy $E = 6.5$ GeV. In real experiment, however, the beam is not monoenergetic. This was taken into account in preparing Fig. 2.5 where oscillation probabilities were convoluted with the energy spectra of the MINOS+ experiment (Fig. 1.1). The vertical lines in Fig. 2.5 mark the L/E regions for Near (ND) and Far (FD) MINOS+ detectors. The Near Detector is located at the distance 1 km from the neutrino source where three-flavour oscillations are not expected, while Far Detector is situated 735 km away, in the region of maximum oscillations. In the absence of sterile neutrinos, the probability that at any L muon neutrino will be detected as one of the active neutrinos is always equal to the unity.
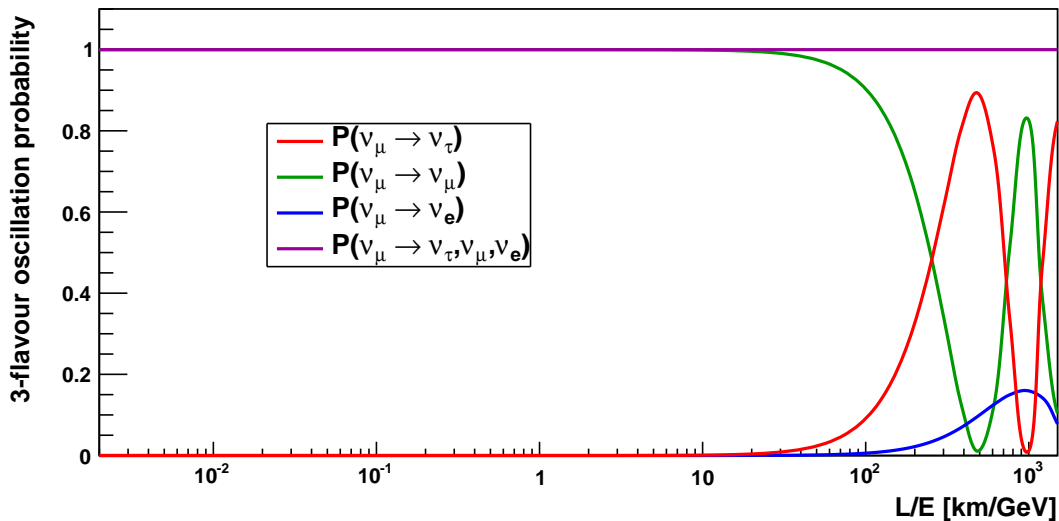
Figure 2.4. Three-flavour neutrino oscillation probabilities as a function of L/E for monoenergetic beam of energy $E = 6.5$ GeV corresponding to the mean reconstructed energy of charged-current, CC ν_μ interactions in the MINOS+ detectors. Values of Δm^2_{32}, Δm^2_{21}, θ_{12}, θ_{13} and θ_{23} from [122].
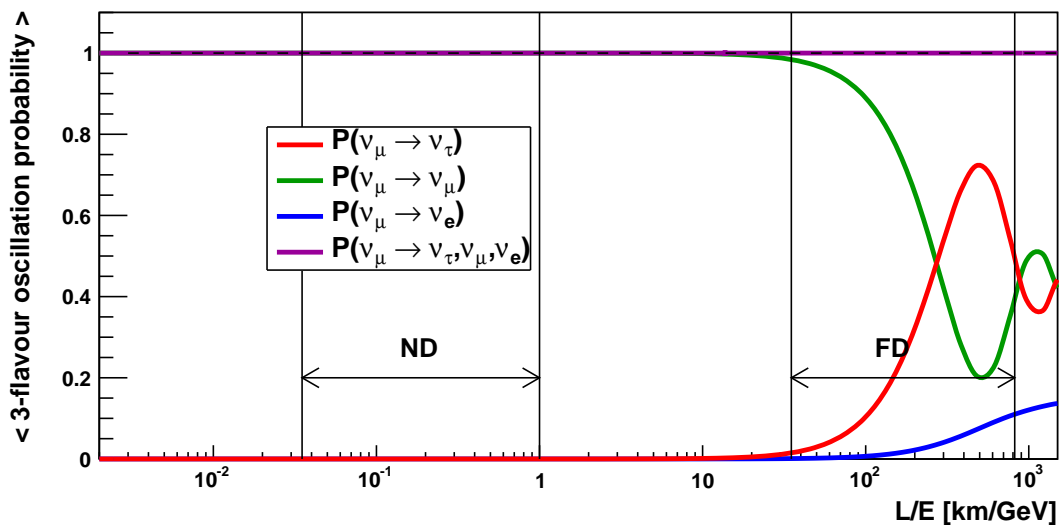

Figure 2.5. Three-flavour neutrino oscillation probabilities as a function of L/E for non-monoenergetic beam. Probabilities were convoluted with MINOS+ energy distribution. Values of Δm^2_{32}, Δm^2_{21}, θ_{12}, θ_{13} and θ_{23} from [122]. Vertical lines mark the L/E regions for Near (ND) and Far (FD) MINOS+ detectors.

2.2. Sterile neutrinos

The name *sterile neutrino* was introduced by Bruno Pontecorvo in 1967 [101]. It is a neutral lepton that does not take part in the weak interactions, but can mix with known active neutrinos ν_e, ν_μ or ν_τ. However, it is not excluded that it takes part in Yukawa interactions involving the Higgs boson or in the new physics interactions.

Sterile neutrino fields are introduced in many extensions of the Standard Model that provide neutrino mass generation mechanism. These fields are fundamentally different from other fermion fields, as they are invariant under the Standard Model symmetries: they are $SU(3)_C \times SU(2)_L \times U(1)_Y$ singlet fields. The usual convention is to call the sterile neutrino fields "right-handed", to distinguish them from the Standard Model neutrino fields, which participate in the weak interactions through

their left-handed chiral components. There are neither limits on number of sterile neutrinos nor on their mass. Therefore, there are three active, left-handed neutrinos ν_{eL}, $\nu_{\mu L}$, $\nu_{\tau L}$ and in general, there can be N_s sterile right-handed neutrinos $\nu_{s_1 R}, \ldots \nu_{N_{sR}}$.

It is not possible to observe the interactions of sterile neutrinos, but they can influence neutrino oscillations. In the presence of N_s sterile neutrinos, the oscillation mixing matrix has to be extended to the size $(3 + N_s) \times (3 + N_s)$ (Eq. (2.25))

$$\mathbf{U} = \begin{pmatrix} U_{e1} & U_{e2} & U_{e3} & U_{e4} & \ldots \\ U_{\mu 1} & U_{\mu 2} & U_{\mu 3} & U_{\mu 4} & \ldots \\ U_{\tau 1} & U_{\tau 2} & U_{\tau 3} & U_{\tau 4} & \ldots \\ U_{s1} & U_{s2} & U_{s3} & U_{s4} & \ldots \\ \vdots & \vdots & \vdots & \vdots & \ddots \end{pmatrix} . \tag{2.25}$$

Expression on the transition $\nu_\alpha \to \nu_\beta$ in vacuum in the model with sterile neutrinos is the same as for three-flavour oscillations (Eq. (2.15)) described in Section 2.1. The formula would hold for any number of neutrino flavours.

If sterile neutrinos exist, the mixing between sterile and active neutrino states must be small and the new massive neutrinos must be mostly sterile in order not to spoil the very good agreement of data from neutrino experiments with the three-neutrino oscillation model:

$$|U_{\alpha i}|^2 \ll 1 \qquad\qquad (\alpha = e, \mu, \tau; i = 4, \ldots, N). \tag{2.26}$$

The experiments that study disappearance of ν_e or $\overline{\nu}_e$ can probe the elements from the first row of the neutrino mixing matrix, $|U_{ei}|$. Similarly, the ν_μ or $\overline{\nu}_\mu$ disappearance experiments set limits on $|U_{\mu i}|$. In comparison, appearance experiment in the channel $\nu_\alpha \to \nu_\beta$ is sensitive to the elements from two rows of the mixing matrix: $|U_{\alpha i}|$ and $|U_{\beta i}|$. In particular, limits on the mixing of ν_τ with the sterile states ($|U_{\tau i}|$) can be obtained in the ν_τ appearance experiments that search for the anomalous appearance of tau neutrinos in the beam of muon neutrinos and from the data involving neutral-current (NC) interactions that allow to distinguish between $\nu_\mu \to \nu_\tau$ and $\nu_\mu \to \nu_s$ oscillations. There are many data sets that are used to set bounds on $|U_{e4}|^2$ and $|U_{\mu 4}|^2$. On the contrary, only limited number of data can be used to constrain $|U_{\tau 4}|^2$ and the corresponding limits are not tight. Therefore, the possible mixing of active neutrino states with sterile neutrinos can be the largest in the tau neutrino sector.

2.3. Neutrino masses

Neutrinos can oscillate only if they have non-zero masses, but in the Standard Model of strong and electroweak interactions they are strictly massless. Therefore, after the discovery of neutrino oscillations the theory had to be extended to describe neutrino mass generation [45, 129]. There are numerous extensions of the Standard Model and many of them predict existence of right-handed neutrino fields. Therefore, the hypothesis of sterile neutrino is theoretically well motivated.

Dirac masses

The simplest possibility to introduce neutrino mass is the generation of Dirac neutrino mass with the same Higgs mechanism that is responsible for masses of other leptons and quarks in the Standard Model. In this approach, the new right-handed neutrino fields that are singlets under the SM symmetries have to be introduced. The number of right-handed neutrino fields is not constrained by

the theory, but the introduction of three right-handed fields would create, to a certain level, symmetry between quark and lepton sectors. In such a case, the Higgs-lepton Yukawa Lagrangian can be written as

$$\mathscr{L}_{\mathrm{H,L}} = -\sum_{\alpha=\mathrm{e,\mu,\tau}} \frac{y_\alpha^l v}{\sqrt{2}} \bar{l}_\alpha l_\alpha - \sum_{k=1}^{3} \frac{y_k^\nu v}{\sqrt{2}} \bar{\nu}_k \nu_k - \sum_{\alpha=\mathrm{e,\mu,\tau}} \frac{y_\alpha^l}{\sqrt{2}} \bar{l}_\alpha l_\alpha \mathrm{H} - \sum_{k=1}^{3} \frac{y_k^\nu}{\sqrt{2}} \bar{\nu}_k \nu_k \mathrm{H}, \tag{2.27}$$

where ν_k stands for Dirac neutrino fields

$$\nu_k = \nu_{k\mathrm{L}} + \nu_{k\mathrm{R}} \qquad (k = 1,2,3) \tag{2.28}$$

l_α for charged lepton fields

$$l_\alpha = l_{\alpha\mathrm{L}} + l_{\alpha\mathrm{R}} \qquad (\alpha = \mathrm{e,\mu,\tau}), \tag{2.29}$$

and H for Higgs field. Charged leptons and Dirac neutrinos couple to the Higgs field through the third and the last term in Eq. (2.27), correspondingly. First and second terms are mass terms with neutrino masses given by

$$m_k = \frac{y_k^\nu v}{\sqrt{2}}, \tag{2.30}$$

and masses of charged leptons defined as

$$m_\alpha = \frac{y_\alpha^l v}{\sqrt{2}}, \tag{2.31}$$

where v is the vacuum expectation value of Higgs field. The experimental limits on neutrino masses [1] show that neutrino masses are a few orders of magnitude smaller than those of all other fundamental particles, including electron. Therefore, in Dirac approach the values of the Higgs-neutrino Yukawa couplings y_k^ν have to be much smaller than y_α^l couplings of charged leptons with the Higgs and the origin of huge difference in masses of charged and neutral leptons remains unknown.

Majorana masses

There is an interesting possibility that neutrinos are Majorana particles. In such a case Majorana fields of massive neutrinos

$$\nu_k = \nu_{k\mathrm{L}} + \nu_{k\mathrm{L}}^{\mathrm{c}}, \tag{2.32}$$

satisfy the condition

$$\nu_k^c = \nu_k, \tag{2.33}$$

where ν_k^c is the charge conjugated field. In case of three generations of massive Majorana neutrinos, the Majorana Lagrangian mass term can be written as:

$$\mathscr{L}_{\mathrm{mass}}^{\mathrm{Majorana}} = \frac{1}{2} \sum_{k=1}^{3} m_k \nu_{k\mathrm{L}}^{\mathrm{T}} \mathcal{C}^\dagger \nu_{k\mathrm{L}} + \mathrm{H.c.}, \tag{2.34}$$

where $\mathcal{C}$ is the unitary charge-conjugation matrix, with $\mathcal{C}\gamma_\mu^{\mathrm{T}}\mathcal{C}^{-1} = -\gamma_\mu$ and $\mathcal{C}^{\mathrm{T}} = -\mathcal{C}$ or as

$$\mathscr{L}_{\mathrm{mass}}^{\mathrm{Majorana}} = -\frac{1}{2} \sum_{k=1}^{3} m_k \bar{\nu}_{k\mathrm{L}}^{\mathrm{c}} \nu_{k\mathrm{L}} + \mathrm{H.c.} \tag{2.35}$$

Dirac–Majorana mass term

It is known that the ν_L exist, because neutrinos take part in the SM weak interactions. If there are no ν_R, the only possible mass term in the Lagrangian is the Majorana mass term (for simplicity only one neutrino generation, ν_L and ν_R, is considered here):

$$\mathscr{L}_{\text{mass}}^{\text{L}} = \frac{1}{2} m_L \nu_L^T \mathcal{C}^\dagger \nu_L + \text{H.c.} \tag{2.36}$$

However, if ν_R exists as well, the Lagrangian can additionally contain Dirac mass term ($\nu = \nu_L + \nu_R$):

$$\mathscr{L}_{\text{mass}}^{\text{D}} = -m_D \overline{\nu}\nu = -m_D(\overline{\nu}_R \nu_L + \overline{\nu}_L \nu_R) = -m_D \overline{\nu}_R \nu_L + \text{H.c.} \tag{2.37}$$

and Majorana mass term for ν_R

$$\mathscr{L}_{\text{mass}}^{\text{R}} = -\frac{1}{2} m_R \nu_R^T \mathcal{C}^\dagger \nu_R + \text{H.c.} \tag{2.38}$$

Therefore, in general it is possible that Dirac and Majorana terms are both present. If one defines column matrix of left-handed neutrino fields

$$\mathbf{N}_L = \begin{pmatrix} \nu_L \\ \nu_R^c \end{pmatrix} = \begin{pmatrix} \nu_L \\ \mathcal{C}\overline{\nu}_R^T \end{pmatrix}, \tag{2.39}$$

and uses the relation $\overline{\nu}_L^c = -\nu_L^T \mathcal{C}^\dagger$, the Dirac–Majorana mass term can be written as

$$\mathscr{L}_{\text{mass}}^{\text{M+D}} = \mathscr{L}_{\text{mass}}^{\text{L}} + \mathscr{L}_{\text{mass}}^{\text{R}} + \mathscr{L}_{\text{mass}}^{\text{D}} = \frac{1}{2} \mathbf{N}_L^T \mathcal{C}^\dagger \mathbf{M} \mathbf{N}_L + \text{H.c.}, \tag{2.40}$$

where $\mathbf{M}$ is a symmetric mass matrix

$$\mathbf{M} = \begin{pmatrix} m_L & m_D \\ m_D & m_R \end{pmatrix}. \tag{2.41}$$

In order to find the mass eigenstates one has to diagonalize the mass matrix with a unitary transformation

$$\mathbf{N}_L = \mathbf{U}\mathbf{n}_L, \tag{2.42}$$

where $\mathbf{n}_L$ is a column matrix of left-handed massive neutrino fields:

$$\mathbf{n}_L = \begin{pmatrix} \nu_{1L} \\ \nu_{2L} \end{pmatrix}. \tag{2.43}$$

The unitary matrix $\mathbf{U}$ is such that

$$\mathbf{U}^T \mathbf{M} \mathbf{U} = \begin{pmatrix} m_1 & 0 \\ 0 & m_2 \end{pmatrix}, \tag{2.44}$$

with real and positive m_i. After the transformation defined in Eq. (2.42), the Dirac–Majorana term from Eq. (2.40) can be written as

$$\mathscr{L}_{\text{mass}}^{\text{M+D}} = \frac{1}{2} \sum_{k=1,2} m_k \nu_{kL}^T \mathcal{C}^\dagger \nu_{kL} + \text{H.c.} = -\frac{1}{2} \sum_{k=1,2} m_k \overline{\nu}_k \nu_k, \tag{2.45}$$

with the massive Majorana neutrino field:

$$\nu_k = \nu_{k\mathrm{L}} + \nu_{k\mathrm{L}}^{\mathrm{c}} = \nu_{k\mathrm{L}} + \mathcal{C}\overline{\nu}_{k\mathrm{L}}^{\mathrm{T}}. \tag{2.46}$$

Therefore, in the general case massive neutrinos are Majorana particles. There are, however, several special cases:

- The pure Dirac case, $m_{\mathrm{L}} = m_{\mathrm{R}} = 0$, where pair of Majorana fields form a Dirac neutrino.
- The pseudo-Dirac case, $m_{\mathrm{D}} \gg |m_{\mathrm{L}}|, m_{\mathrm{R}}$, with small shift between masses and $m_{2,1} \simeq m_{\mathrm{D}} \pm \frac{m_{\mathrm{L}} + m_{\mathrm{R}}}{2}$.
- The see-saw case, $m_{\mathrm{D}} \ll m_{\mathrm{R}}, m_{\mathrm{L}} = 0$ that leads to a heavy, mostly sterile state ν_1 with $m_1 \simeq m_{\mathrm{R}}$ and a very light, mostly active state ν_2 with mass $m_2 \simeq \frac{m_{\mathrm{D}}^2}{m_{\mathrm{R}}}$. The see-saw mechanism thus provides the good explanation of smallness of neutrino masses.
- The pure Majorana case, $m_{\mathrm{D}} = 0$, when there is no mixing between the active and sterile neutrino states.

The mass matrix and Lagrangian mass terms can be generalized for the bigger number of neutrinos, where number of sterile neutrinos does not have to be equal three. For the three active left-handed flavour neutrino fields $\nu_{\mathrm{eL}}, \nu_{\mu\mathrm{L}}, \nu_{\tau\mathrm{L}}$ and N_{s} sterile right-handed flavour neutrino fields, after diagonalization of the mass matrix, the Dirac–Majorana Lagrangian mass term takes the form

$$\mathscr{L}_{\mathrm{mass}}^{\mathrm{M+D}} = -\frac{1}{2} \sum_{k=1}^{N} m_k \overline{\nu}_k \nu_k, \tag{2.47}$$

where $N = 3 + N_{\mathrm{s}}$.

2.4. Oscillations between active and sterile neutrino states

The simplest model that includes sterile neutrinos is the model with 3 active neutrinos and 1 sterile neutrino, called further 3+1 model. The mixing matrix is then a 4×4 unitary matrix with 9 parameters: 6 mixing angles and 3 oscillation-relevant CP-violating phases. In addition to the three known mixing angles $\theta_{12}, \theta_{23}, \theta_{13}$ and one CP-violating phase $\delta \equiv \delta_1$, the 3+1 model introduces three new mixing angles $\theta_{14}, \theta_{24}, \theta_{34}$ and two phases δ_2 and δ_3. The presence of one additional massive neutrino leads to the three new mass-squared differences: Δm_{41}^2, Δm_{42}^2, and Δm_{43}^2, but only one of them is independent of the mass-squared differences of the three-flavour model. The results of the MINOS and MINOS+ sterile analyses are presented as a function of Δm_{41}^2.

In the accelerator experiments, mixing with sterile neutrinos would be seen in certain regions of L/E as a depletion of charged-current (mediated by W boson) CC ν_{μ} and neutral-current (mediated by Z boson) NC events or anomalous appearance of ν_{τ} or ν_e events. Example of the 3+1 oscillation probabilities as a function of L/E, for neutrino energy $E = 6.5$ GeV, $\Delta m_{41}^2 = 10$ eV^2, $\theta_{14} = 0.2$, $\theta_{24} = 0.2$, $\theta_{34} = 0.6$, $\delta_i = 0$, with matter effects included is shown in Fig. 2.6. Values of Δm_{32}^2, Δm_{21}^2, θ_{12}, θ_{13} and θ_{23} were taken from [122]. Contrary to the three-flavour oscillations, the probability of transformation of ν_{μ} from accelerator into an active neutrino of any flavour does not have to be equal to the unity. The fact that neutrino beam is non-monoenergetic makes the oscillation probabilities in a function of L/E look smoother (Fig. 2.7) than in the ideal, monoenergetic case (Fig. 2.6). Similarly as in Fig. 2.5, in the Fig. 2.7 oscillation probabilities were convoluted with the energy spectra of the MINOS+ experiment. The vertical lines mark the MINOS+ L/E regions, while black arrows indicate L/E value corresponding to the maximum rate of events in the Near and Far MINOS+ detectors. The set of Figs. 2.8, 2.9, 2.10 and 2.11 demonstrate the effect of changes of Δm_{41}^2 on the neutrino flux observed in the two detectors of the MINOS+ experiment, for the same example values of mixing angles not excluded by the existing data, as in Figs. 2.6 and 2.7.